Biosensors and Bioelectronics 26 (2011) 2619–2625

Contents lists available at ScienceDirect

Biosensors and Bioelectronics

journal homepage: www.elsevier.com/locate/bios

Development of an electrochemical DNA biosensor with a high sensitivity of fM by dendritic gold nanostructure modified electrode

Feng Li*, Xiaoping Han, Shufeng Liu*

State Key Laboratory Base of Eco-Chemical Engineering, College of Chemistry and Molecular Engineering, Qingdao University of Science and Technology, Qingdao 266042, People's Republic of China

ARTICLE INFO

Article history:
Received 9 August 2010
Received in revised form
14 November 2010
Accepted 15 November 2010
Available online 21 November 2010

Keywords:
DNA immobilization
DNA hybridization
Dendrite gold nanoparticle
Electrochemical biosensor

ABSTRACT

In this paper, dendritic gold nanostructure (DenAu) modified electrode was obtained by direct electrodeposition of planar electrode into 2.8 mM $HAuCl_4$ and 0.1 M H_2SO_4 solution under a very negative potential of −1.5 V. Scanning electron microscopy was used to characterize the growth evolution of DenAu with time. The whole DNA biosensor fabrication process based on the DenAu modified electrode was characterized by cyclic voltammetry and electrochemical impedance spectroscopy methods with the use of ferricyanide as an electrochemical redox indicator. The probe DNA immobilization and hybridization with target DNA on the modified electrode could be well distinguished by using methylene blue as an electrochemical hybridization indicator. The DenAu modified electrode could realize an ultra sensitivity of 1 fM toward complementary target DNA and a very wide dynamic detection range (from 1 fM to 1 nM).

1. Introduction

In recent years, the development of highly sensitive and selective DNA biosensors has been received ever increasing attentions in connection with efforts directed at gene analysis, the detection of genetic disorders, tissue matching, forensic and more medical applications (Taton et al., 2000; Gunnarsson et al., 2008). In contrast to many existing techniques for DNA detection such as fluorescence (Yang et al., 2008; Duan et al., 2007), surface plasmon resonance spectroscopy (Kim et al., 2007) and quartz crystal microbalance (Patolsky et al., 2000; Minunni et al., 2005), electrochemical technique affords a lot of advantages such as its simplicity, rapidness, low-cost and high sensitivity (Drummond et al., 2003; Liu et al., 2008; Zhang et al., 2009a,b; Li et al., 2010). Different strategies have been devoted for the electrochemical detection of DNA hybridization. The electroactive indicators are commonly used as redox labels for electrochemical detection of DNA hybridization (Munde et al., 2007; Gorodetsky et al., 2008).

In pursuit to achieve DNA electrochemical detection with a high sensitivity, nanostructures with different morphology have been advised for the modification of substrate aiming at increasing the immobilization amount of probe DNA and improving the recognition property of immobilized DNA (Kjällman et al., 2008; Hill et al., 2009; Liu et al., 2010a). Over the last several years, very high sensitivities have been demonstrated based on nanomaterial-based electrochemical assays. For example, Kelley research group fabricated controlled nanowire and Pd nanostructures modified electrodes and achieved sensitive DNA detection through controlling the orientation of probe DNA (Gasparac et al., 2004; Soleymani et al., 2009a). The detection limit toward target DNA for this nanostructured electrode was estimated to be approximately 1.0 fM. Chang et al. (2007) fabricated an electrochemical DNA biosensor based on conducting polyaniline nanotube array and could readily detect the target DNA at a concentration as low as 1.0 fM. Hu et al. (2008) prepared a nanoporous electrode by a dealloying strategy and developed an electrochemical sensitive DNA biosensor with the combination of a signal amplification technology of DNA–Au bio bar code. This approach offered a detection limit as low as 28 aM toward target DNA. Liu et al. (2005) prepared the nanogold aggregates modified electrode and could realize a detection limit of 10 pM toward target DNA with the use of methylene blue (MB) as an electrochemical indicator. Chang et al. (2008) developed an electrochemical DNA biosensor based on palladium nanoparticles combined with carbon nanotubes and the detection limit for the detection of target DNA was obtained as 0.12 pM. The introduction of nanomaterial could efficiently increase the electrode surface area and enlarge the DNA immobilization amount. Furthermore, the nanostructure may play an important role in the orientation and assembly density control of probe DNA for the optimized hybridization recognition ability. Whereas, these reported nanostructures are usually involved into comparatively complex preparation procedures or the signal amplification effect for the

* Corresponding authors. Tel.: +86 532 84023927; fax: +86 532 84023927.
E-mail addresses: lifeng@qust.edu.cn (F. Li), sliu@qust.edu.cn (S. Liu).

0956-5663/$ – see front matter © 2010 Elsevier B.V. All rights reserved.
doi:10.1016/j.bios.2010.11.020

DNA electrochemical detection is limited. Thus, the construction of nanostructure modified electrode by a simple strategy to achieve the electrochemical DNA detection with a high sensitivity is highly desirable.

The gold nanostructures modified electrode could be easily constructed by some different strategies including direct electrostatic assembly, covalent linking, polymer entrapment or co-mixing, sol–gel, and electrodeposition methods. Among them, electrodeposition method is one of the mostly used approaches with the advantages of convenience and the wide applications in electrocatalysis and electroanalysis. Till now, different morphologies of gold nanostructures have been obtained by electrodeposition including spherical, pinlike, flowerlike, etc. (Li and Shi, 2005; Tian et al., 2006). For example, Zhang et al. (2004), obtained a dendritic gold aggregate by electrodeposition on a polyelectrolyte multilayer matrix modified ITO electrode. Zhang et al. (2008) fabricated various gold nanostructures on glassy carbon electrodes in a low concentration of 5 mM $HAuCl_4$ solution by electrodeposition method. Wang and co-workers prepared a hierarchical flowerlike gold microstructure with gold nanoplates or nanopricks as building blocks by electrochemical deposition in a high concentration of 24.3 mM $HAuCl_4$ without introducing any template or surfactant (Guo et al., 2007). Xu et al. (2010) obtained a dendritic gold nanostructure by a templateless, surfactantless, simple electrochemical route and studied its application to oxygen reduction. Chen et al. (2009) fabricated a three-dimensional gold film electrode by direct electrodeposition method and studied the direct electrochemistry and electrocatalysis of hemoglobin onto it. The development of hierarchical gold nanostructures by simple electrodeposition method is very attractive for the applications in biosensor, electrocatalysis, etc. Even though there are a lot of research works involved in the development of different gold nanostructures for the performance improvement of biosensor, the role of nanostructuring in modulating biodetection sensitivity has been less addressed and needs further explore in detail (Soleymani et al., 2009b).

In this article, a dendritic gold nanostructure (DenAu) modified electrode was prepared by a very simple direct electrodeposition strategy. The electrodeposition of gold nanostructures was operated by applying a negative potential of −1.5 V into 2.8 mM $HAuCl_4$ and 0.1 M H_2SO_4 solution. The hydrogen gas bubble was observed out across the electrode surface following the whole electrodeposition process. This could be attributed to the formation of DenAu. The DenAu modified electrode was further used to fabricate DNA biosensor using methylene blue (MB) as an electrochemical indicator and a very low detection limit of 1 fM toward complementary target DNA could be achieved (Lin et al., 2007; Jin et al., 2007; Zhang et al., 2009a,b). It is also convinced that the current study should be easily extended to the more applications for example in protein, enzyme biosensor.

2. Experimental

2.1. Chemicals and materials

Tetrachloroaurate(III) tetrahydrate ($HAuCl_4{\cdot}4H_2O$, 47.8% Au) were obtained from National Chemical Reagent Co. Ltd. (Shanghai, China). 6-Mercaptohexanol, methylene blue (MB) was purchased from Sigma–Aldrich (St. Louis, MO, USA). $K_3Fe(CN)_6$, $K_4Fe(CN)_6$ were purchased from Tianjin Ruijinte Chemical. Co. Ltd. (Tianjin, China). All other chemicals were of analytical grade and used without further purification. Doubly distilled water (18.2 MΩ) was used throughout the experiment.

All of synthetic oligonucleotides were purchased from SBS Genetech. Co. Ltd. (Beijing, China). Their base sequences are listed as follows:

Probe DNA: 5′-SH-GCG CGA ACC GTA TA-3′
Complementary target DNA: 5′-TAT ACG GTT CGC GC-3′
Non-complementary target DNA: 5′-ACT GAT GCT ACC AT-3′

2.2. Apparatus

Cyclic voltammetry (CV) and differential pulse voltammetry (DPV) measurements were performed with a CHI832B electrochemical analyzer (Shanghai, China). Electrochemical impedance spectroscopy (EIS) measurements were carried out on a CHI660C electrochemical workstation (Shanghai, China). All electrochemical experiments were performed with a conventional three-electrode system comprising a gold working electrode, a platinum wire auxiliary electrode, and a Ag/AgCl reference electrode. The EIS measurements were performed in 1.0 mM $K_3[Fe(CN)_6]$ containing 0.10 M KCl with the frequency range from 10^5 to 0.1 Hz. The scanning electron microscopy (SEM) measurements of the modified electrode surfaces were performed on a Hitachi S-4300 scanning electron microscope (Japan).

2.3. Preparation of dendritic gold nanostructure (DenAu) modified electrode

The planar gold electrode surface was freshly polished prior to use with 0.05 μm alumina powder and then cleaned ultrasonically sequentially in acetone and water for 3 min. The electrode was then subjected to electrochemical pretreatment by consecutive potential cycling in a 0.5 M H_2SO_4 solution within a potential window between −0.2 and +1.5 V at a scan rate of 100 mV s^{-1} until a stable reproducible voltammogram was obtained. The DenAu electrodeposition on the pretreated planar gold electrode was conducted at −1.5 V in a stationary 2.8 mM $HAuCl_4$ and 0.1 M H_2SO_4 solution (without stirring or N_2 bubbling) for different time.

2.4. DNA biosensor fabrication

The immobilization of thiolated probe DNA on planar or DenAu modified electrode was performed with the immersion of electrode in 0.1 μM probe DNA solution in PBS (0.1 M, pH 7.4) for 12 h. Then the modified electrode was further immersed into the blank PBS buffer for 1 h at 37 °C with stirring. This operation was used to eliminate the non-specific adsorbed probe DNA molecule on the electrode surface. The probe DNA immobilized electrode was then immersed into 1 mM MCH aqueous solution to further eliminate the non-adsorbed DNA molecules and to hold a good orientation of probe DNA for its good recognition ability. Then the electrodes were taken out and rinsed with PBS buffer solution and doubly distilled water and dried with nitrogen. The hybridization experiments were carried out by immersing the probe DNA modified electrode into different concentration of target DNA (complementary or non-complementary) in PBS (0.1 M, pH 7.4) at 37 °C for 1 h. And then, the hybridized electrodes were rinsed with PBS buffer solution and water and then dried with nitrogen.

2.5. DNA hybridization detection with an electrochemical indicator of methylene blue

The probe DNA or hybridized electrodes were firstly immersed into 1 mM MB in 0.1 M PBS (pH 7.4, 0.1 M KCl) for 20 min, and then the cyclic voltammograms (CV) and differential pulse voltammograms (DPV) were recorded in blank 0.1 M PBS (pH 7.4) solution.

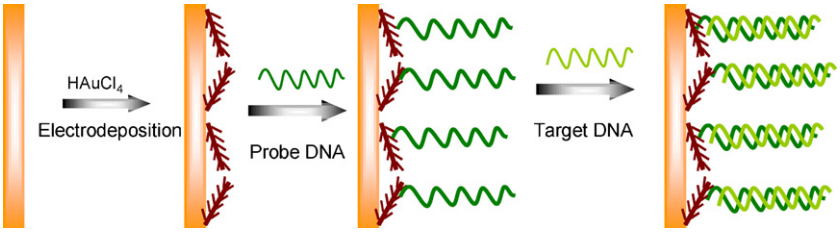

Fig. 1. Schematic illustration of the fabrication steps of the electrochemical DNA biosensor.

3. Results and discussions

3.1. Preparation of DenAu modified electrode

Schematic representation of the fabrication procedure of DNA biosensor is shown in Fig. 1. The DenAu modified electrode was firstly prepared by an electrochemical deposition strategy and then used as the substrate for DNA immobilization and hybridization. In order to obtain a three-dimensional gold film with porous structure in electrochemical deposition, the deposition potential was set at −1.5 V where a large amount of hydrogen bubbles were evolved. Fig. 2 shows the SEM images of obtained DenAu electrode at −1.5 V for 600 s. The lower magnification image (Fig. 2A) demonstrates that the product consists of a large amount of dendritic nanostructures. The width of these dendritic nanostructures is several hundred nanometers and the length is up to about 3 μm. There are also some small pieces and rod-like nanostructures. High-magnification images (Fig. 2B) reveal the detail of this dendritic gold nanostructure. The nanostructure is symmetrical to the bone-axis, and composed of small nanoparticles, which is similar to other reports (Xu et al., 2010). The relative surface area could be evaluated from the coulombic integration of the reductive waves of gold oxide formed in the positive potential scan in 0.5 M H_2SO_4 (Fig. 2C) (Trasatti and Petrii, 1992). It could be deduced that the surface area of DenAu modified electrode is about 8.3 times compared with that of planar gold electrode. Whereas, the surface area increase for the common gold nanoparticles electrodeposited electrode is only about 2–4 times compared with that of planar gold electrode (Liu et al., 2010b). This further indicated that the current obtained DenAu modified electrode took a three-dimensional porous nanostructure and largely increased the effective electrode surface area.

To understand the formation mechanism of dendritic nanostructure, the relationship between the morphology and reaction time was inspected. Fig. 3 shows the morphology of the dendritic nanostructure with different reaction time. From Fig. 3A–D, one can figure out that there is a tendency that the nanostructure grows more and more complex when reaction time increases. At 20 s reaction time, the electrode surface was observed to be occupied by densely packed irregular nanoparticles (Fig. 3A). Furthermore, the nanoparticles on the electrode surface could be simply differentiated with top layer (light dots) and bottom layer (dark dots). The nanoparticles of top layer seem to always form circle-like structure with deep observation. This could be attributed to the growth of gold nanoparticles is templated by formed small hydrogen gas bubbles at the initial stage. When the reaction time is prolonged to be 100 s, the rod-like nanoparticle with a sharp tip becomes formed (Fig. 3B). This indicated that the subsequent growth of gold crys-

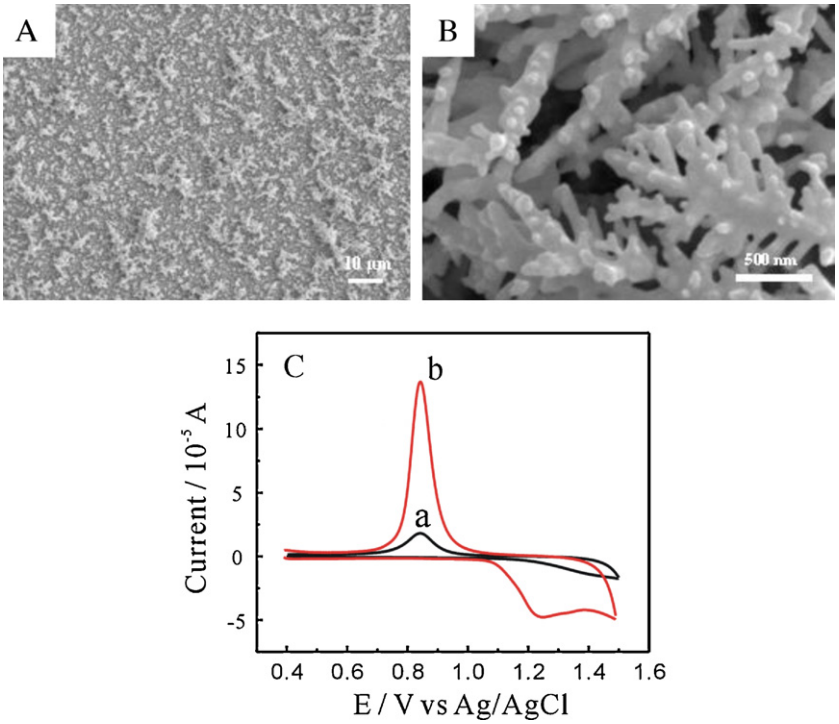

Fig. 2. (A) Low and (B) high magnification SEM images of prepared DenAu electrode by electrodeposition in 2.8 mM $HAuCl_4$ and 0.1 M H_2SO_4 solution at −1.5 V for 600 s; (C) cyclic voltammogram of the planar gold (a) and obtained DenAu (b) electrodes in 0.5 M H_2SO_4 solution at a scan rate of 100 mV s^{-1}.

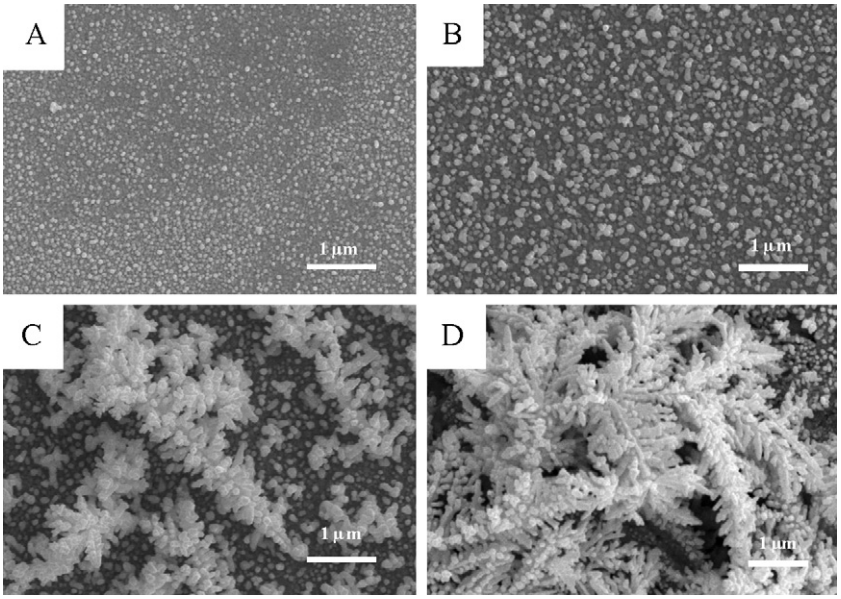

Fig. 3. SEM images of the obtained DenAu electrodes by electrodeposition in 2.8 mM $HAuCl_4$ and 0.1 M H_2SO_4 solution at −1.5 V for different times: (A) 20 s, (B) 100 s, (C) 300 s, and (D) 600 s.

tals would preferentially occur on the preformed gold nuclei. The as-prepared nanostructure becomes dendritic at 300 s (Fig. 3C) and the dendritic structure becomes larger and more symmetrical at 600 s (Fig. 3D). The formation of the nanostructure experienced a growth of the nanoparticle to a 3D dendritic nanostructure. The hydrogen bubble evolved during the electrodeposition process acted as a dynamic template to assist the orientation growth of gold nanocrystal. The electrochemical deposition of gold always occurred on the existing gold nuclei, which evolved into the final dendritic nanostructure (Xu et al., 2010).

3.2. Electrochemical behaviors of $[Fe(CN)_6^{3-/4-}]$ at the modified electrode surface

Fig. 4A shows the cyclic voltammograms obtained for differently modified electrodes in 1 mM $[Fe(CN)_6^{3-/4-}]$ and 0.1 M KCl solution at the scan rate of 100 mV s^{-1}. A pair of well-defined redox peaks was observed on the bare gold electrode with the anodic (E_{pa}) and cathodic (E_{pc}) peak potential of 0.23 V and 0.12 V, respectively (curve a). After the electrodeposition of DenAu, the peak current of $[Fe(CN)_6^{3-/4-}]$ increased and the peak to peak potential separation (ΔE_p) decreased slightly (curve b), indicating a better redox behaviors of $[Fe(CN)_6^{3-/4-}]$ on the DenAu modified electrode. After probe DNA and MCH immobilization on the DenAu modified electrode, the peak current of $[Fe(CN)_6^{3-/4-}]$ was largely inhibited and the ΔE_p was largely increased (curve c). This could be easily explained by the limited diffusion of $[Fe(CN)_6^{3-/4-}]$ toward electrode surface by the negative charged phosphate backbone of probe DNA. A further decreased peak current and increased ΔE_p was observed after hybridization of probe DNA with target complementary DNA (curve d). This could be well assigned that the introduction of complementary DNA increases the negative charge responsible for the increased repellence of redox species.

EIS could provide further information on the impedance changes of the electrode surface during the modification process. In EIS, the semicircle diameter could represent the electron-transfer resistance, R_{et}, which dominate the electron transfer kinetics of the redox probe at the electrode interface. Fig. 4B shows the Nyquist plot of the differently modified electrodes in 1 mM $Fe(CN)_6^{3-}/Fe(CN)_6^{4-}$ and 0.1 M KCl at open circuit potential with the frequency varied from 0.1 Hz to 100 kHz. The planar gold electrode witnessed a small R_{et} value of about 1200 Ω (curve a). After DenAu modification, an almost straight line was observed, indicating an improvement of electron transfer ability of $[Fe(CN)_6^{3-/4-}]$ by the modified DenAu. The R_{et} was increased to be about 1.5×10^4 Ω with the self-assembly of probe DNA and MCH on the electrode surface (curve c). The R_{et} value was further increased to be about 2.5×10^4 Ω after hybridized with complementary target DNA. The R_{et} increase after probe DNA immobilization and hybridization could be well ascribed to the repellence of redox probe from approaching electrode surface by negative charged phosphate skeletons of DNA. The results of impedance experiments were in good agreement with that of cyclic voltammetry experiments.

3.3. The selectivity of electrochemical DNA biosensor

Fig. 5A shows the cyclic voltammograms of the DNA modified DenAu electrodes measured in blank PBS buffer solution after immersion in 1 mM MB of 0.1 M PBS (pH 7.4, 0.1 M KCl) for 20 min. A pair of well-defined redox peaks of MB could be observed with the formal potential at −0.21 V and a very small ΔE_p value of about 10 mV (curve a). This could be attributed to the redox reaction of MB confined at the ssDNA chains by an electrostatic interaction mode. A good linear relationship of peak current with scan rates ranged from 30 mV to 300 mV could be obtained, indicating a very well surface controlled redox behaviors of MB at the probe DNA immobilized electrode (data not shown for brief). A significant increase of MB peak current was observed after hybridization with complementary target DNA (curve c). The control experiments performed with the hybridization of probe DNA with non-complementary target DNA showed almost the same response with that of only ssDNA modified electrode (curve b), indicating that MB could be used as a good indicator to selectively detect the target DNA (Kara et al., 2002; Li et al., 2007; Zhang et al., 2009a,b). The intercalation interaction of MB with dsDNA is considered to play a major role for the increased current responses of dsDNA than that of ssDNA (Kelley et al., 1997; Li et al., 2007; Taft et al., 2006). Also, more binding amount of MB by an electrostatic interaction at the dsDNA chain than that at ssDNA may contribute to the increased current responses of dsDNA.

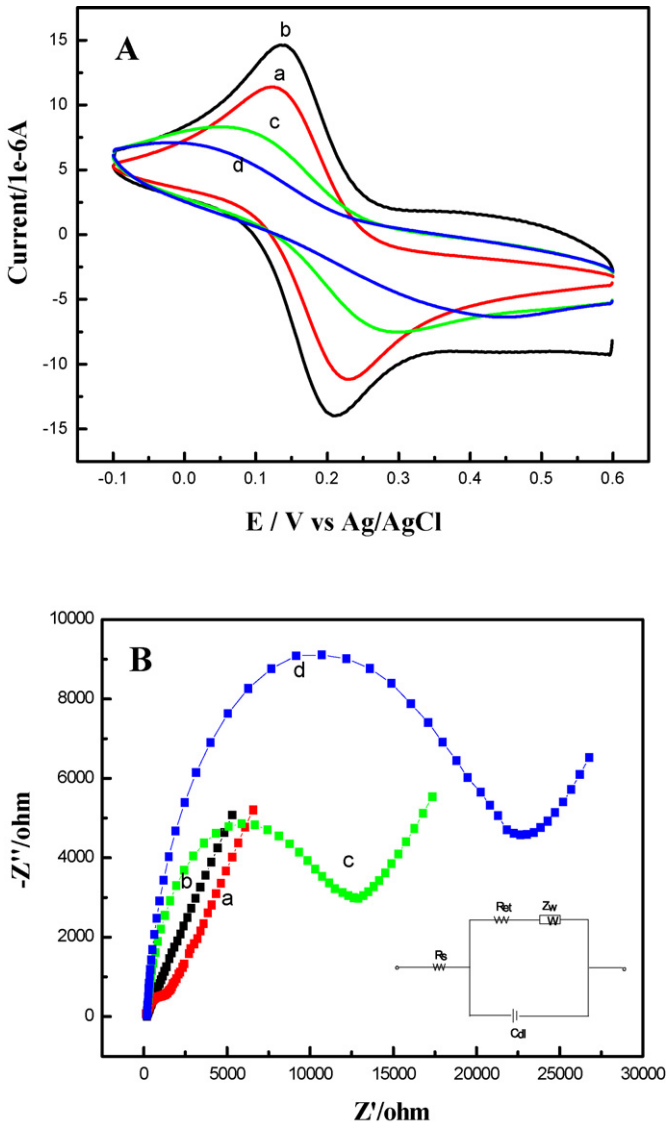

Fig. 4. (A) Cyclic voltammograms and (B) the Nyquist plots obtained for bare (a), DenAu modified (b), thiolated ssDNA and MCH immobilized (c), and hybrized with complementary target DNA modified (d) electrodes at 100 mV s^{-1} in 1 mM $[Fe(CN)_6^{3-/4-}]$ and 0.1 M KCl solution. The concentration of complementary target DNA were 1 nM in PBS (0.1 M, pH 7.4).

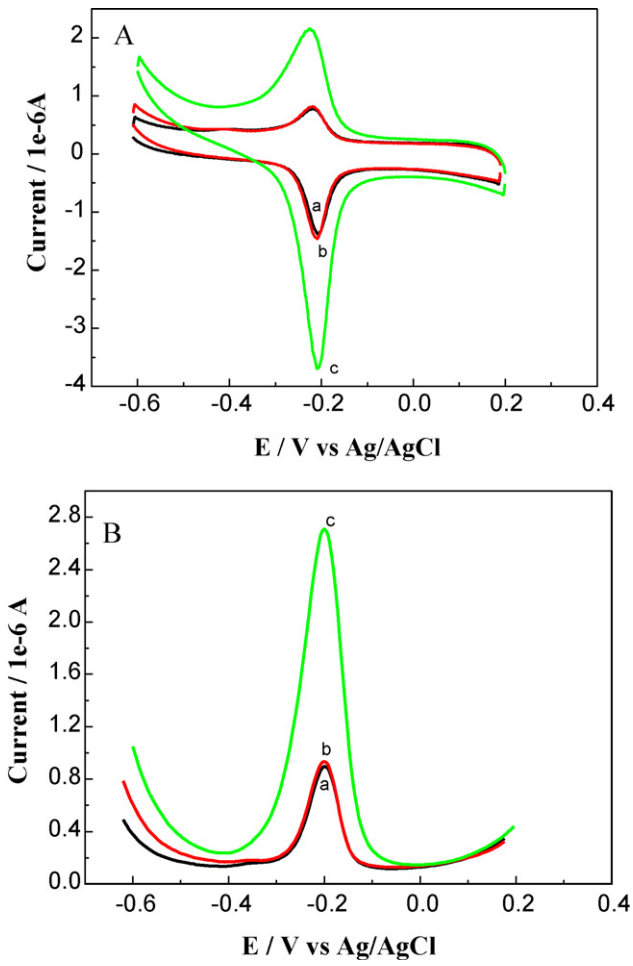

Fig. 5. (A) Cyclic voltammograms and (B) differential pulse voltammograms of ssDNA immobilized (a), hybrids with target DNA (c) and non-complementary target DNA sequence (b) modified electrodes in blank PBS buffer solution after immersion in 1 mM MB of 0.1 M PBS (pH 7.4, 0.1 M KCl) for 20 min. The concentrations of complementary and non-complementary target DNA were both 1 nM in PBS (0.1 M, pH 7.4). The scan rates were all 100 mV s^{-1}.

The DPV experiments using MB as an electrochemical hybridization label for detection of DNA sequences were further advised and the results were shown in Fig. 5B. A peak current of MB of 0.9 μA was obtained at the ssDNA modified DenAu electrode (curve a). An increase of about 1.84 μA in the DPV signal was observed after hybridization with fully complementary target DNA (curve c). Whereas, almost the same peak current with the solely probe DNA immobilized electrode was obtained when recognition with non-complementary target DNA (curve b). The DPV experiments showed a high selectivity of the constructed DNA biosensor for hybridization detection and the MB could be used as a good electrochemical indicator to properly discriminate the ssDNA and dsDNA by our fabricated strategy, which was in good accordance with that of cyclic voltammetry experiments. The DPV peak current increase of MB (ΔI_p) before and after hybridization with target DNA (1 nM) could be simply used to characterize the hybridization amount with target DNA. The ΔI_p value of MB on the different DenAu electrodes obtained at deposition time of 20 s, 100 s, 300 s, 600 s were about 0.23 ± 0.04, 0.42 ± 0.07, 0.82 ± 0.12, 1.84 ± 0.11 μA, respectively. This strongly indicated that the amount and morphology of DenAu has a major effect on the amount of immobilized probe DNA and thus DNA detected. The increase of hybridization amount was more evident than the increase of electrode surface area. The selective determination of current fabricated DNA biosensor toward one-base mismatched and two-base mismatched target DNA was also studied (see Fig.S2 in the Supplementary Information). It strongly indicated a good selectivity of current fabricated DNA biosensor toward complementary, non-complementary and mismatched target DNA sequences.

3.4. The sensitivity of fabricated DNA biosensor

The DPV peak current increase before and after hybridization of probe DNA with complementary target DNA was further used to evaluate the performance of current DNA biosensor fabricated on the DenAu modified electrode. It could be seen from Fig. 6A that the DPV peak current of MB on the DenAu electrode increases with the increasing target DNA concentration ranged from 1 fM to 1 nM. In Fig. 6B, the peak current change of fabricated DNA sensor exhibited a linear correlation to the logarithm of the target DNA concentration ranged from 1 fM to 1 nM with a linear regression coefficient of 0.998. The low detection limit was obtained as 1 fM (S/N = 3), which are much higher or comparable with that of current many nano-

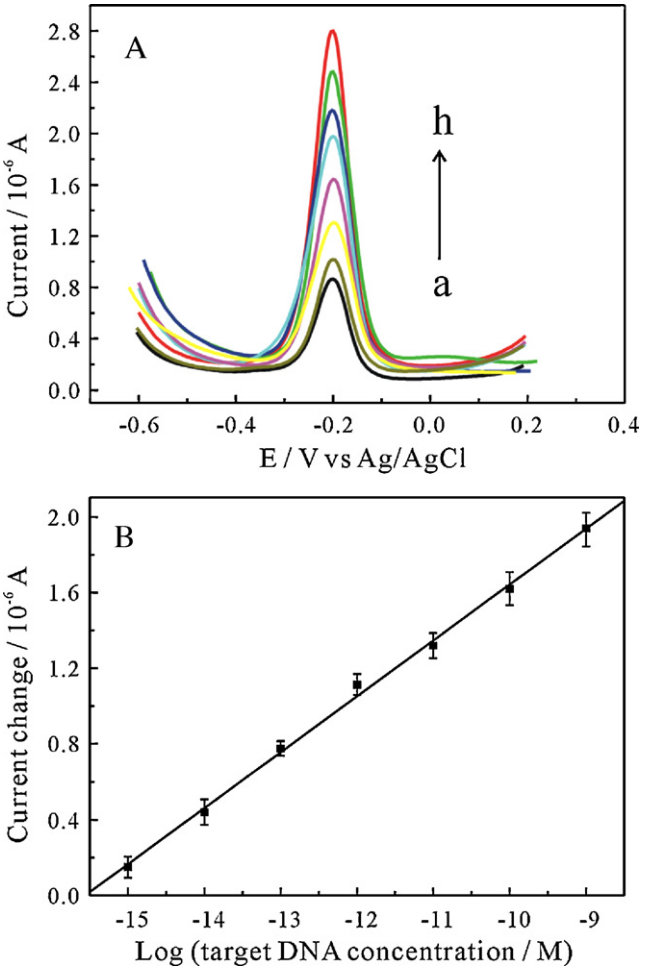

Fig. 6. (A) The DPV responses of MB for different DNA hybrids. Concentration of target DNA: (a) 0 M, (b) 1×10^{-15} M, (c) 1×10^{-14} M, (d) 1×10^{-13} M, (e) 1×10^{-12} M, (f) 1×10^{-11} M, (g) 1×10^{-10} M, and (h) 1×10^{-9} M. (B) Linear relationship between the DPV peak current change and the logarithm of the target DNA concentration.

materials modified electrodes (see Tab.S1 in the Supplementary Information). Four independent electrodes were used simultaneously for the acquisition of each point in the calibration curve. The DenAu with a huge surface area was considered to supply numerous attaching points for probe DNA immobilization. And also, the immobilization orientation and assembly density of probe DNA may be well controlled by three-dimensional dendritic structure of DenAu for optimized hybridization efficiency. On the other side, the hierarchical three-dimensional dendritic structure in present case may diminish the repelling behavior when approaching of the target DNA toward the immobilized probe DNA and enhance the hybridization efficiency. But the role of DenAu in the sensitivity improvement is not still very clear and needs further study in detail in the future.

3.5. Regeneration and stability of the fabricated DNA biosensor

Regeneration is useful for continuous monitoring of the target DNA in future research. It was found that the fabricated DNA biosensor could be regenerated 6 times with about 18% loss of the original signal by dipping the electrode in hot water (80 °C) for 10 min, followed by a rapid cooling in an ice bath for 10 min. The signal attenuation seemed to be attributed to the loss of thiolated probes on the DenAu electrode surface. At the same time, the stability of the fabricated DNA biosensor was investigated. The probe DNA modified electrode was firstly stored in the refrigerator at 4 °C over 2 weeks and then examined via DPV after its hybridization with complementary target DNA. Experiments demonstrated that the DNA biosensor retained about 91% of its initial response.

4. Conclusions

An electrochemical DNA biosensor based on the DenAu modified electrode was constructed for the sensitive detection of a short DNA sequence. The developed electrode largely increases the electrode surface area, which is about 8.3 times compared with that of planar gold electrode. The special three-dimensional dendritic nanostructure of DenAu is likely beneficial to increase the immobilization amount of probe DNA and further hybridization amount with target DNA. With the use of MB as an indicator, the optimized DNA biosensor could achieve a wide linear range from 1 fM to 1 nM for the target DNA detection and a low detection limit of 1 fM. The current fabricated DNA biosensor should be also suitable for the detection of target DNA in real samples, for example clinical analytes. Moreover, this electrode modification strategy was expected for further extensive applications in protein, enzyme biosensors.

Acknowledgements

This research was supported by the National Natural Science Foundation of China (Nos. 20775039, 21005043), and the Natural Science Foundation of Shandong Province of China (Nos. Q2008B05, ZR2009BM031, ZR2009BM013).

Appendix A. Supplementary data

Supplementary data associated with this article can be found, in the online version, at doi:10.1016/j.bios.2010.11.020.

References

Chang, H., Yuan, Y., Shi, N., Guan, Y., 2007. Anal. Chem. 79, 5111–5115.
Chang, Z., Fan, H., Zhao, K., Chen, M., He, P., Fang, Y., 2008. Electroanalysis 20, 131–136.
Chen, Y., Yang, X.-J., Guo, L.-R., Li, J., Xia, X.-H., Zheng, L.-M., 2009. Anal. Chim. Acta 644, 83–89.
Drummond, T.G., Hill, M.G., Barton, J.K., 2003. Nat. Biotechnol. 21, 1192–1199.
Duan, X., Li, Z., He, F., Wang, S., 2007. J. Am. Chem. Soc. 129, 4154–4155.
Gasparac, R., Taft, B.J., Lapierre-Devlin, M.A., Lazareck, A.D., Xu, J.M., Kelley, S.O., 2004. J. Am. Chem. Soc. 126, 12270–12271.
Gorodetsky, A.A., Buzzeo, M.C., Barton, J.K., 2008. Bioconjug. Chem. 19, 2285–2296.
Gunnarsson, A., Jönsson, P., Marie, R., Tegenfeldt, J.O., Höök, F., 2008. Nano Lett. 8, 183–188.
Guo, S.J., Wang, L., Wang, E.K., 2007. Chem. Commun., 3163–3165.
Hill, H.D., Millstone, J.E., Banholzer, M.J., Mirkin, C.A., 2009. ACS Nano 3, 418–424.
Hu, K., Lan, D., Li, X., Zhang, S., 2008. Anal. Chem. 80, 9124–9130.
Jin, Y., Yao, X., Liu, Q., Li, J., 2007. Biosens. Bioelectron. 22, 1126–1130.
Kara, P., Kerman, K., Ozkan, D., Meric, B., Erdem, A., Ozkan, Z., Ozsoz, M., 2002. Electrochem. Commun. 4, 705–709.
Kelley, S.O., Barton, J.K., Jackson, N.M., Hill, M.G., 1997. Bioconjug. Chem. 8, 31–37.
Kim, D., Kerman, K., Saito, M., Sathuluri, R.R., Endo, T., Yamamura, S., Kwon, Y., Tamiya, E., 2007. Anal. Chem. 79, 1855–1864.
Kjällman, T.H.M., Peng, H., Soeller, C., Travas-Sejdic, J., 2008. Anal. Chem. 80, 9460–9466.
Li, Y., Shi, G.Q., 2005. J. Phys. Chem. B 109, 23787–23793.
Li, D., Yan, Y., Wieckowska, A., Willner, I., 2007. Chem. Commun. 34, 3544–3546.
Li, H., Sun, Z., Zhong, W., Hao, N., Xu, D., Chen, H.-Y., 2010. Anal. Chem. 82, 5477–5483.
Lin, X.-H., Wu, P., Chen, W., Zhang, Y.-F., Xia, X.-H., 2007. Talanta 72, 468–471.
Liu, S., Li, Y., Li, J., Jiang, L., 2005. Biosens. Bioelectron. 21, 789–795.
Liu, G., Wan, Y., Gau, V., Zhang, J., Wang, L., Song, S., Fan, C., 2008. J. Am. Chem. Soc. 130, 6820–6825.
Liu, S., Liu, J., Han, X., Cui, Y., Wang, W., 2010a. Biosens. Bioelectron. 25, 1640–1645.
Liu, S., Liu, J., Wang, L., Zhao, F., 2010b. Bioelectrochemistry 79, 37–42.
Minunni, M., Tombelli, S., Fonti, J., Spiriti, M.M., Mascini, M., Bogani, P., Buiatti, M., 2005. J. Am. Chem. Soc. 127, 7966–7967.
Munde, M., Ismail, M.A., Arafa, R., Peixoto, P., Collar, C.J., Liu, Y., Hu, L., David-Cordonnier, M., Lansiaux, A., Bailly, C., Boykin, D.W., Wilson, W.D., 2007. J. Am. Chem. Soc. 129, 13732–13743.
Patolsky, F., Lichtenstein, A., Willner, I., 2000. J. Am. Chem. Soc. 122, 418–419.

Soleymani, L., Fang, Z., Sargent, E.H., Kelley, S.O., 2009a. Nat. Nanotechnol. 4, 844–848.
Soleymani, L., Fang, Z., Sun, X., Yang, H., Taft, B.J., Sargent, E.H., Kelley, S.O., 2009b. Angew. Chem. Int. Ed. 48, 8457–8460.
Taft, B.J., Lapierre-Devlin, M.A., Kelley, S.O., 2006. Chem. Commun., 962–964.
Taton, T.A., Mirkin, C.A., Letsinger, R.L., 2000. Science 289, 1757–1760.
Tian, Y., Liu, H.Q., Zhao, G.H., Tatsuma, T., 2006. J. Phys. Chem. B 110, 23478–23481.
Trasatti, S., Petrii, O.A., 1992. J. Electroanal. Chem. 327, 353–376.
Xu, X., Jia, J., Yang, X., Dong, S., 2010. Langmuir 26, 7627–7631.
Yang, R., Jin, J., Chen, Y., Shao, N., Kang, H., Xiao, Z., Tang, Z., Wu, Y., Zhu, Z., Tan, W., 2008. J. Am. Chem. Soc. 130, 8351–8358.
Zhang, X., Shi, F., Yu, X., Liu, H., Fu, Y., Wang, Z., Jiang, L., Li, X., 2004. J. Am. Chem. Soc. 126, 3064–3065.
Zhang, H., Xu, J.-J., Chen, H.-Y., 2008. J. Phys. Chem. C 112, 13886–13892.
Zhang, S., Wu, Z., Shen, G., Yu, R., 2009a. Biosens. Bioelectron. 24, 3201–3207.
Zhang, Y., Wang, Y., Wang, H., Jiang, J., Shen, G., Yu, R., Li, J., 2009b. Anal. Chem. 81, 1982–1987.